Mechanism underlying dynamic size effect on rock mass strength

Chengzhi Qi[a,*], Mingyang Wang[b], Jiping Bai [c], Kairui Li[a]

[a]Beijing Research Center for Engineering Structures and New Materials, Beijing University of Civil Engineering and Architecture, Beijing 100044, China

[b]Civil Engineering Institute, PLA University of Science and Technology, Nanjing 210007, China

[c]Faculty of Computing, Engineering & Science, University of South Wales, Pontypridd, CF37 1DL, UK

Abstract: This paper presents the research on mechanism of dynamic size effect on rock mass strength based on structural hierarchy. Relaxation model of Maxwell type for rock mass is used to obtain the relationship between strength, sample size and strain rate. This model is used to analyse the experimentally observed laws of dynamic size effect on rock mass strength. It is shown that because of the finitness of crack propagation velocity, when the strain rate is well above certain charateristic strain rate, dynamic loading process takes predominant role. The stresses in sample have not enough time to relax completely. The larger the sample size is, the more time is required for cracks to propagate through the sample, and the higher the applied stresses are before the macrofractures of samples occur. On the other hand because of the static size effect the higher dynamically applied stresses will initiate the cracking at smaller scale levels of rock sample, and the fragment size is smaller. The developed model succeeded in explaining the main features of dynamic and static size effect and the apparent controversy in experimental data, and in predicting the dynamic fragmentation size, the characteristic transition strain rate and characteristic sample size.

Key words: rock mass strength, dynamic size effect, static size effect, structural hierarchy

1. Introduction

The strength of rock-like materials is size-dependent, i.e. the strength of a rock sample varies in sample size. The size-dependent strength of rock-like materials at quasi-static loading condition has been studied by many scientists. According to research carried out by Bazant [1], size effect on strength can be classified into two types: (1) statistical mechanism, described by the Weibull theory of randomness of local material strength [2-4] and (2) energetic (deterministic) mechanism including type I size effect [5-10] for materials with failure initiation from an undamaged smooth surface, and type II size effect [5, 11-14] for materials with a pre-existing notch (or stress-free crack) formed stably before reaching the maximum load. Another approach to size effect study is based on the concept of fractality or self-similarity. The fractality of concrete deformation and fracture was examined by Bazant [7] and Carpinteri et al [15, 16] while the mechanics of hierarchical materials was also developed [17].

Research into the size effect on the dynamic strength of rock-like materials is limited.

Collaborative studies [18-20] have been conducted to assess the effect of time on the size effect in concrete cylindrical specimens under compressive impact. Four different sizes of concrete cylinders were studied (diameter×height): 75×150, 150×300, 300×600, 600×1200mm. The impact velocities used were 5 and 7 m/s. The corresponding strain rates varied in the range of 0.06-3.03s^{-1} for normal concrete cylinders, and 0.014-0.111 s^{-1} for high strength concrete cylinders. Experimental data indicate that size effect existed for compressively loaded concrete cylinders under dynamic loads. Generally, as the size of the specimen increased, the apparent strength decreased.

Hong et al.[21] performed refined research about the size and strain-rate effects on the dynamic strength of rock. The testing results show that the rock dynamic strength increases with strain-rate in power law which agree with the findings by other scientists [22-25]. The interesting result is that the larger the specimen size is, the more notable the strain-rate sensitivity of dynamic strength of rock is, i.e. the rock dynamic strength increases with the increase of

* Corresponding author. Tel./fax: t+86 10 68322492, +8613701328772 (mobile).
E-mail addresses: qichengzhi65@163.com, qichengzhi@bucea.edu.cn (C. Qi).

specimen size under the same strain-rate which is opposite to the size effect under static loading condition (see Fig.1 and 2 for granite). The size effect of dynamic strength becomes weaker with the decrease of strain-rate and there exist a critical strain-rate below which static size effect takes dominant position. In addition, experiments show that the size of the fragments decreases significantly with the increase of sample size. The smaller the sample size is, the bigger the dispersion of the experimental results is.

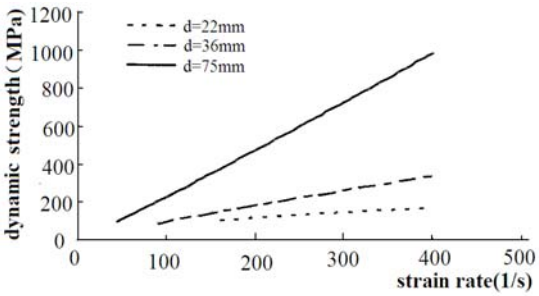

Fig. 1 Strain-rate effect on dynamic strength of rocks with different specimen diameters [21]

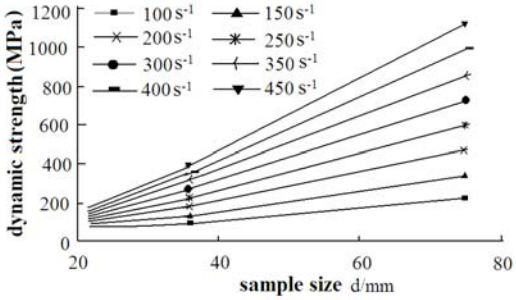

Fig. 2 Sample size effect on dynamic strength of rocks under various strain-rates [21]

For a given strain-rate, the larger the sample size is, the smaller the fragment size is, as shown in Fig.3.

(a) d=75mm, $\dot{\varepsilon} = 98.23s^{-1}$ (b) d=36mm, $\dot{\varepsilon} = 99.75s^{-1}$ (c) d=22mm, $\dot{\varepsilon} = 164.38s^{-1}$

Fig.3 Fragmentation of granite specimens with different sizes under different strain-rates [21]

The experimental investigation on size effect of rock dynamic fracture toughness was performed by Wang et al [26] using four geometrically similar holed-cracked flattened Brazilian disc specimens with diameter of 42 mm、80 mm、122 mm and 155 mm respectively. The discs were diametrically impacted at the flat end by the split Hopkinson pressure bar of 100 mm diameter. Experiments showed that the rock dynamic fracture toughness increases with the diameter for the geometrically similar specimens; under the same loading rate, the larger the sample size is, the more noticeable the dynamic effect is. Gunsallus and Kulhawy [27], Bhagat [28], Whittaker et al. [29], and Zhang et al [30] found some approximate relations between fracture toughness and tensile strength, compressive strength etc. on the basis of experimental data from literature. Generally, the tensile strength, compressive strength of rock are proportional to fracture toughness. Therefore the experimental results obtained by Wang et al [26] comply with those of Hong et al [21].

Liang et al [31] reported the static and quasi-dynamic tests on granite specimens under various strain rates using rock dynamic loading system. The specimens were 50 mm in diameter, with the lengths of 50，75，100，125 mm，respectively. The experimental data showed that under static and quasi-dynamic loading conditions (with strain rates of 10^{-5}～10^{-2} s^{-1})，rock strength generally decreases with the increase in specimen length.

The above mentioned experimental data clearly show certain controversy.

What is the underlying mechanism of dynamic size effect on rock mass strength? What is the relationship between static and dynamic size effects? May the above mentioned controversial experimental data be interpreted within one unified theoretical framework? This paper presents a theoretical study and examines the underlying mechanism of dynamic size effect on rock mass strength from the viewpoint of structural hierarchy.

2. Mechanism underlying dynamic size effect on rock mass strength

Rock is a natural material and has complex internal structure with a wide range of scales. In-situ investigations [32] as well as experimental and theoretical studies [33] showed that the deformation and fracture of rock-like materials are governed by the laws of Maxwell bodies and can be described using Maxwell model. Why are the mechanical behaviors of rock-like materials governed by the laws of Maxwell bodies? The reason is that rock-like materials are quasi-brittle materials, in deformation and fracture process plastic deformations in rock-like materials are not significant, the deformation and fracture process of rock-like materials is mainly governed by elastic deformations and cracking.

The internal structure of rocks has decisive influence on the mechanical behavior of rocks. The crystals with ideal regular lattices have their theoretical strength, but the strength of real materials is about 2-3 orders lower than the theoretical strength of the ideal crystals. Obviously, the complex hierarchic internal structure of real materials causes the stress concentration and strain localization which are responsible for the reduction of real material strength.

As a reference medium, a crystal with ideal regular lattices will be considered. When such ideal crystal is subjected to intensive external loading, the intensity of which is high enough, but well below the strength limit, then damage, fracture and stress relaxation will not occur in the crystal. But if the ideal crystal is replaced by a real rock mass with complex internal structure, then stress concentration, successive damage and fracture would occur under the action of such intensive external loading. Consequently, part of the stresses in rock mass will be relaxed. Therefore, the stress may be divided into two components, i.e. the elastic stress caused by the reversible dilatational and distortional deformations, and the local inelastic stress due to structural heterogeneities or internal structure which are responsible for the irreversible deformations. The elastic stress is related to the reversible deformation linearly. The residual stress (inelastic stress) Δs_{ij}^{l} arises at definite strain-rate and relaxes with time. The evolution equation for the residual deviatoric stresses Δs_{ij}^{l} due to structural heterogeneities may be described by Maxwell model

$$\frac{d\Delta s_{ij}^{l}}{dt} = 2\rho c_s^2 \dot{e}_{ij} - v\frac{\Delta s_{ij}^{l}}{l} \qquad (1)$$

where Δs_{ij}^{l} is the residual deviatory stress components in structural heterogeneities with characteristic scale l; $\dot{e}_{ij}$ is the corresponding strain-rate components, ρ is the density of the medium; v is the relaxation velocity, which may be interpreted as the propagation velocity of single or multiple cracks depending on the loading conditions; c_s is the propagation velocity of the elastic shear wave. Here it is assumed that all residual stress components relax with the same relaxation time. Essentially l/v may be considered as relaxation time $\tau = l/v$. The first term on the right-hand side of Eq.(1) describes the elastic loading, while the second term on the right-hand side of Eq.(1) depicts stress relaxation due to cracking.

The main feature of this model is that, the relaxation rate of the residual stresses in structural heterogeneities is

proportional to the magnitude of the residual stresses, and inversely proportional to the size of the structural heterogeneities. The growth of residual stresses is controlled by two contradicting factors on the right-hand side of Eq.(1), i.e. the stress growth rate $2\rho c_s^2 \dot{e}_{ij}$ and the relaxation rate of residual stresses $v\Delta s_{ij}^l / l$. It is necessary to note that this model is applicable not only to different rock-like materials with great variation range of relaxation times, but also to highly viscous fluids for which the relaxation time is relatively short [34].

For constant strain rate the solution of Eq. (1) has the following form

$$\Delta s_{ij}^l = 2\rho c_s^2 \dot{e}_{ij} \frac{l}{v}\left[1 - e^{-vt/l}\right] = 2\rho c_s^2 \dot{e}_{ij}\tau\left[1 - e^{-t/\tau}\right] \tag{2}$$

For short loading time $t << \tau$, relaxation process has not enough time to develop, and the loading process is the predominant factor, in this case Eq.(2) gives

$$\Delta s_{ij}^l \approx 2\rho c_s^2 \dot{e}_{ij} t = 2\rho c_s^2 e_{ij} \tag{3}$$

i.e. the residual stress will increase almost linearly with time.

For long loading time $t >> \tau$, relaxation process has enough time to develop and the loading is influenced by the relaxation, therefore, Eq.(2) gives

$$\Delta s_{ij}^l \approx 2\rho c_s^2 \dot{e}_{ij}\tau = 2\rho c_s^2 \dot{e}_{ij} \frac{l}{v} \tag{4}$$

For the occurrence of macroscopic fracture, it is necessary that the loading time is greater than relaxation time $t > \tau$, therefore Eq.(4) is appropriate for the study of macroscopic fracture of rock samples.

Define the intensity of residual deviatory stress as $\Delta\sigma_I = \sqrt{3\Delta s_{ij}^l \Delta s_{ij}^l / 2}$ and substituting Eq.(4) into it, we obtain

$$\Delta\sigma_I = 3\rho c_s^2 \dot{\varepsilon}_I \frac{l}{v} \tag{5}$$

where $\dot{\varepsilon}_I = \sqrt{2\dot{e}_{ij}\dot{e}_{ij}/3}$ is the intensity of the strain-rate.

It can be seen from Eqs.(4) and (5) that if the applied strain-rate is fixed, then the larger the size of the heterogeneous structural elements is, the greater the residual stresses are. Therefore, we introduce the sample size (*D*) into the model. The main cause of the material fracture is the residual stresses due to stress concentration near heterogeneous structural elements. When the intensity of residual stresses $\Delta\sigma_I$ reaches the strength σ_Y of the sample, fracture occurs. Therefore Eq.(5) may be rewritten as

$$\sigma_Y = 3\rho c_s^2 \dot{\varepsilon}_I \frac{D}{v} \quad . \tag{6}$$

Equation (6) explicitly shows that dynamic strength is proportional to the size of sample, and inversely proportional to the the relaxation velocity. The physical mechanism can be explained as follows.

Experiments show that the maximum crack growth velocity is limited by the Rayleigh wave speed C_R [35]. Therefore, the relaxation velocity is also limited. The larger the sample size is, the longer it is needed for the occurrence of macroscopic fracture, thus, the higher the ultimate load can be achieved. Factually, dynamic strength enhancement of rock sample is the overloading induced by the delay of fracture due to the finiteness of the fracture propagation velocity.

Now the dynamic size effect can be explained. For granite, Young's modulus of $E = 5.5\times10^{10} Pa$ and

Poisson's ratio of $\mu = 0.29$ can be used (thus, the corresponding shear modulus is $G = 2.13 \times 10^{10} Pa$). For samples with sizes of $D = 22mm = 0.022m$, $D = 36mm = 0.036m$ and $D = 75mm = 0.075m$, the effective relaxation velocities according to Eq.(6) are $v = 3515m/s$, $v = 2465m/s$ and $v = 1867m/s$, respectively, when the experimental data shown in Figs.(1) and (2) are applied. It is evident that the effective relaxation velocity decreases with the increase of sample size. This relationship is shown in Fig.4 and Eq.(7)

$$v(D) = 112.59D^2 - 1403D + 6056.6 \tag{7}$$

where the unit of D is cm.

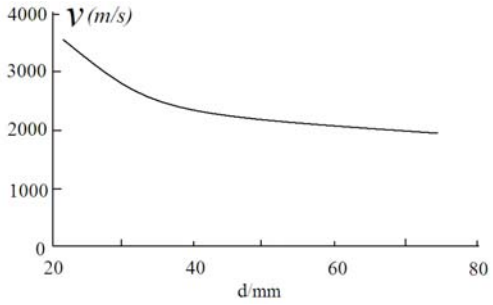

Fig.4 The velocity of crack propagation vs. specimen size

The decrease of relaxation velocity with the increase of sample diameter may be due to the influence of lateral inertial confinement effect induced by the dynamic loading. At high strain rates the inertial confinement becomes very remarkable. In this case there exists a transition from one-dimensional stress to one-dimensional strain [36]. The transition strain rate depends on the material specimen density and the specimen size; the larger the specimen and the higher its density, the lower the transitional strain rate [37, 38]. Li et al.[39, 40] have shown that the apparent concrete cylinder strength could be enhanced significantly at a strain rate beyond 10^2 s^{-1} associated with a significant increase in lateral confinement. Lateral inertial confinement induced by high strain rates delays the macro-fracture of solids and decreases the apparent relaxation velocity.

Thus, the dynamic strength of material can be determined by

$$\sigma_Y = 3\rho c_s^2 \dot{\varepsilon}_I \frac{D}{v(D)} \quad . \tag{8}$$

Eq.(8) fits remarkably well with the experimental data shown in Figs.(1) and (2).

3. The determination of fragment size of rock

The static and dynamic size effect is shown in Fig.5.

The static strength of rock mass depends on the sample size. Generally, the compressive strength of materials σ_Y can be expressed as a function of the sample size *D* as follows [5]

$$\sigma_Y = \sigma_0 (1 + D/D_0)^{-1/2} \tag{9}$$

where σ_0 and D_0 are constants. Equation (9) can be rewritten as

$$D = D_0\left[(\sigma_0/\sigma_Y)^2 - 1\right] \tag{10}$$

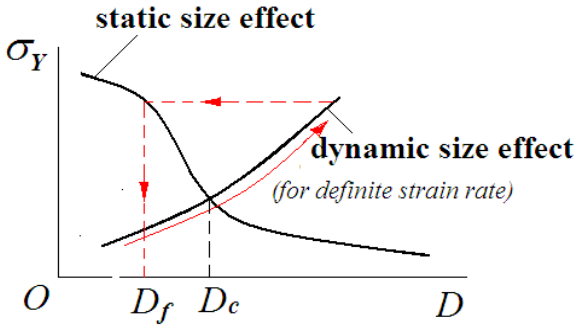

Fig.5 The mechanism of dynamic fragmentation

For fast dynamic loading process, failure will be delayed because of the finiteness of relaxation velocity, and overloading will take place. Therefore, for sufficiently large rock sample, dynamic strength will be higher than static one. Consequently, the higher applied load will activate the deformation and fracture process in rock at smaller scale element levels, and the rock will fracture according to the static size effect law of rock as shown in Fig.5 .

From Eq.(10), following equation is obtained to determine the average dynamic fragment size of fractured rock mass under high strain rates D_f against strain-rate：

$$D_f = D_0\left[\left(\frac{\sigma_0}{\sigma_Y}\right)^2 - 1\right] = D_0\left[\left(\frac{\sigma_0 v(D)}{3\rho c_s^2 \dot{\varepsilon}_I D}\right)^2 - 1\right] \tag{11}$$

where σ_0 and D_0 are determined using the data given in Fig.3(a) and (b). For sample with diameter $d = 75mm$ and strain rate $\dot{\varepsilon} = 98.23s^{-1}$, the dynamic strength is $\sigma_Y = 220MPa$, and the fragment size is approximately $D_f = 0.2cm$. For sample with diameter $d = 36mm$ and strain rate $\dot{\varepsilon} = 99.75s^{-1}$, the dynamic strength is $\sigma_Y = 105MPa$, and the fragment size is approximately $D_f = 1.47cm$. These two sets of data together with Eq.(11) give $D_0 = 1.75mm$ and $\sigma_0 = 3.22\times10^8 Pa$.

Hence,

$$D_f = D_0\left[(\sigma_0/\sigma)^2 - 1\right] = 1.75\times10^{-3}\left[\left(3.22\times10^8/\sigma_Y\right)^2 - 1\right] . \tag{12}$$

For the case shown in Fig.3(c), the diameter of sample is $d = 22mm$. According to Fig.1(a), $\sigma_Y \approx 100MPa$. Substituting $\sigma_Y \approx 100MPa$ into Eq.(14), $D_f = 16.4mm$ is obtained, which is very close to the fragment size in

Fig.3 (c), $D_f \approx 22/\sqrt{2} = 15.6mm$. Therefore, the model can be used to determine the dynamic effects on strength and fragmentation size.

Grady [41, 42] used the model presented in Fig.6 to illustrate the equilibrium and non-equilibrium fragmentation of solids. In the model Grady introduced a term "correlation horizon" to characterize the region of material within which material points are within an elastic distance. In our case the correlation horizon is the size of rock testing samples. In Fig.6 the resisting fragmentation energy curve describes the variation of energy density required to create new fracture surface with the correlation distance. As an example given in [41], the energy density required to fracture a cube of size *l* into equal cubes of size *l*/2 is

$$U_s = 3\Gamma/l \tag{13}$$

where Γ is the fracture surface energy per unit area. It is clear that U_s decreases with increase of l.

The driving fragmentation energy curve describes the dependence of energy density provided by loading process to fuel the fracture process on the correlation horizon. The driving fragmentation energy density is given in [41] and determined by the following equation:

$$U_e = \rho c^2 \dot{\varepsilon}^2 t^2/2 = E\dot{\varepsilon}^2 t^2/2 \tag{14}$$

where U_e represents the elastic energy density induced by dynamic loading before fracture, $\dot{\varepsilon}$ is the strain rate, t is the loading time, and c is the wave propagation velocity. It is clear that U_e increases with the loading time or the correlation distance.

Under condition of $U_e = U_s$, i.e. at the junction of the two energy curves, equilibrium fragmentation is identified [42]. Non-equilibrium fragmentation, in contrast to equilibrium fragmentation, occurs in those materials that, when subjected to dynamic fragmentation conditions, do not fail at the junction of the two energy curves. Instead, elastic strain energy continues to increase until some other failure criterion is achieved.

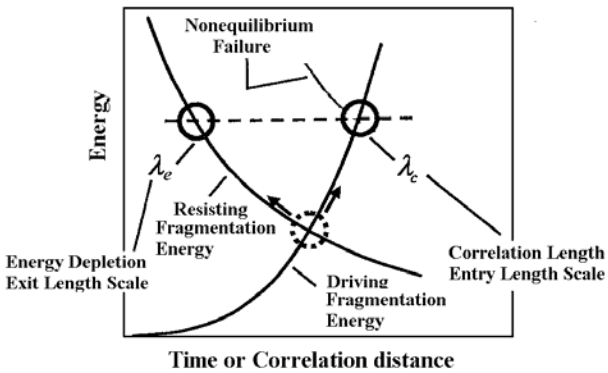

Fig.6 The equilibrium and non-equilibrium fragmentation [41]

It has been found that our proposed model is in good agreement with the model given by Grady.

In Fig.5 following the static size effect curve the energy density required to fracture rock sample is

$$U_f = \frac{\sigma^2(D)}{2E} = \frac{\sigma_0^{\ 2}}{2E(1+D/D_0)} \tag{15}$$

where Eq.(9) is used. It is clear that U_f decreases with the increase of D, and this corresponds to the resisting fragmentation energy curve in Fig.6.

Along the dynamic size effect curve in Fig.5 the energy density provided by loading process to fuel the fracture process is

$$U_e = \rho c^2 \dot{\varepsilon}^2 t^2 / 2 = E\dot{\varepsilon}^2 D^2 / 2v^2 \tag{16}$$

where $t = D/v$ is used. U_e increases with the increase of D, which corresponds to the driving fragmentation energy curve in Fig.6.

When U_e is equal to U_s it reaches the conditions under which equilibrium fragmentation is achieved, and D_c is the average fragment size under equilibrium fragmentation [41, 42]. For the given rock sample size D (corresponding to the entry length scale λ_c in Fig.6) and strain rate $\dot{\varepsilon}$, the average fragment size D_f (corresponding to the exit length scale λ_e in Fig.6) can be determined by using Eq.11. Much of the dynamic fracture and fragmentation mechanism is examined by the length scales D_c and D_f. Onset of failure and initial fracture is governed by the length scale D_c. High strain rates when overloading takes place due to the finiteness of the fracture propagation velocity, results in higher strain energy density. In order to release the excess of the strain energy, crack branching developes. Continued fractures, through successive crack branching, cascade down through the length scales until strain energy is exhausted at the length scale D_f. Over the range of length scales, bounded by D_c and D_f, the behavior of fracture is independent of length scale. The physical processes become self-similarity, and such processes are described by power-law functions of the size d within the range of $D_f < d < D_c$. Hence, our model complies with the model of Grady [41, 42].

4. The determination of characteristic size and characteristic strain rate for rock

For a fixed strain-rate of $\dot{\varepsilon}_I$, assume that there exists a characteristic size D_C for rock sample, above which dynamic size effect on rock strength will predominate. The characteristic size D_C is determined by the intersection of static size effect curve and dynamic size effect curve in Fig.5 by the following relation

$$\sigma_D = \sigma_0 \left(1 + D_c / D_0\right)^{-1/2} = \sigma_Y = 3\rho c_s^2 \dot{\varepsilon}_I \frac{D_c}{v\left(D_c\right)} \tag{17}$$

By substituting Eq.(7) into Eq.(17) we can easily determine the characteristic size D_c.

On the other hand for a fixed rock sample size D, from the following relation

$$\sigma_D = \sigma_0 \left(1 + D / D_0\right)^{-1/2} = \sigma_Y = 3\rho c_s^2 \dot{\varepsilon}_{Ic} \frac{D}{v\left(D\right)} \tag{18}$$

the following characteristic strain-rate can be derived

$$\dot{\varepsilon}_{Ic} = \frac{\sigma_0 v\left(D\right)}{3\rho c_s^2 D\left(1 + D / D_0\right)^{1/2}} = \frac{\sigma_0 v\left(D\right)}{3GD\left(1 + D / D_0\right)^{1/2}} \tag{19}$$

From Eq.(19) it is clear that under fixed rock sample size D, when strain-rate $\dot{\varepsilon} > \dot{\varepsilon}_{Ic}$, dynamic size effect has dominant effect, and when $\dot{\varepsilon} < \dot{\varepsilon}_{Ic}$ static size effect predominates. On the other hand, under fixed strain-rate $\dot{\varepsilon}_{Ic}$, when strain-rate $D > D_c$, dynamic size effect dominates, otherwise static size affects mainly.

From Eq.(19) it is also clear that the larger the specimen and the higher its density, the lower the transitional strain rate. This is in agreement with the findings presented by Forrestal et al. [37], Zhang et al.[38] and Hong et al. [21].

The physical meaning of above conclusion is discussed below.

For rock samples with definite size l, the so-called static strength σ_{st} of rock is measured under definite strain rate $\dot{\varepsilon}_{Ic}$. From the viewpoint of relaxation process, it is meant that in this case loading process is balanced by relaxation process, i.e.

$$\frac{d\Delta s_{ij}^l}{dt} = 2\rho c_s^2 \dot{e}_{ij} - v\frac{\Delta s_{ij}^l}{l} = 0 \tag{20}$$

which means that $\Delta s_{ij}^l = 2\rho c_s^2 \dot{e}_{ij} \frac{l}{v}$, i.e. $\Delta\sigma_I = 3\rho c_s^2 \dot{\varepsilon}_I \frac{l}{v} = \sigma_{st}$. Therefore the corresponding strain rate is $\dot{\varepsilon}_{Ic} = \frac{v\sigma_{st}}{3\rho c_s^2 l}$, indicating that static strength and strain rate have one-to-one correspondence (see Fig.7). When the applied strain rates are greater than $\dot{\varepsilon}_{Ic}, \dot{\varepsilon}_I > \dot{\varepsilon}_{Ic}$, we have $\frac{d\Delta s_{ij}^l}{dt} = 2\rho c_s^2 \dot{e}_{ij} - v\frac{\Delta s_{ij}^l}{l} > 0$, dynamic loading process takes place leading to dominant dynamic size effect (see Fig.7).

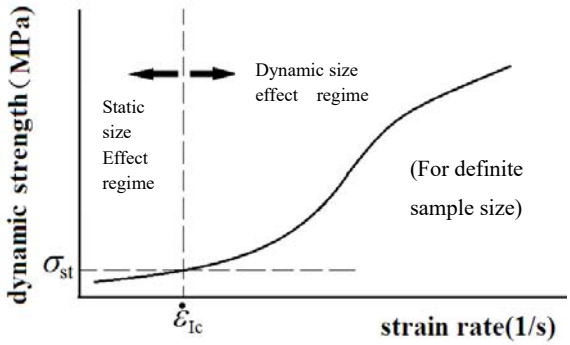

Fig.7 The characteristic transition strain rate

On the other hand, for fixed strain rate $\dot{\varepsilon}$, the corresponding critical sample size satisfying Eq.(20) is $l_{cr}=\frac{\nu\sigma_{st}}{3\rho c_s^2\dot{\varepsilon}_{Ic}}$. If $l>l_{cr}$, then we have $\frac{d\Delta s_{ij}^l}{dt}=2\rho c_s^2\dot{e}_{ij}-\nu\frac{\Delta s_{ij}^l}{l}>0$, which shows that the dynamic size effect occurs (see Fig.5).

The characteristic transition strain-rates for the tests in [21] can be examined using Eq.(19). For sample with diameter $d=75mm$, we have $\nu=1867m/s$, $G=2.13\times10^{10}Pa$, $D_0=1.75mm$, $\sigma_0=3.22\times10^8Pa$, the predicted characteristic transition strain-rate is

$$\dot{\varepsilon}_{Ic}=\frac{\sigma_0\nu(D)}{3GD(1+D/D_0)^{1/2}}=18.9s^{-1}$$

For sample with diameter $d=36mm$, we have $\nu=2645m/s$, and the predicted $\dot{\varepsilon}_{Ic}$ is $\dot{\varepsilon}_{Ic}=74s^{-1}$.

For sample with diameter $d=22mm$, we have $\nu=3515m/s$, and the predicted $\dot{\varepsilon}_{Ic}$ is $\dot{\varepsilon}_{Ic}=227s^{-1}$.

It can be seen from Fig.1 that if the static strength of granite is 70 MPa, the experimentally determined characteristic transition strain-rates for samples with diameters $d=75$, 36 and $22mm$ are $\dot{\varepsilon}_{Ic}=40$, 90 and 160/s, respectively (see Tab.1). With consideration of the experimental errors, the predictions based on the presented model may be regarded as satisfactory.

Table 1

$\dot{\varepsilon}_{Ic}$ determined by experiments and the present model

d	$\dot{\varepsilon}_{Ic}$ (s^{-1}) (by tests)	$\dot{\varepsilon}_{Ic}$ (s^{-1})(by present model)
75mm	40	18.9
36mm	90	74
22mm	160	227

For the case in [18] for high strength concrete cylinders, the elastic modulus is $E=4.72\times10^{10}Pa$, Poisson's ratio

is $\mu = 0.25$, thus, the corresponding shear modulus is $G = 1.89 \times 10^{10} Pa$, the density of the cylinders is $\rho = 2.47 \times 10^3 kg/m^3$. The transverse wave velocity is $C_t = \sqrt{G/\rho} = 2766 m/s$. The Rayleigh wave velocity C_R [43] is $C_R = 0.919 C_t = 2542 m/s$. The size effect law in [18] may be approximated by Eq.(9) with D_0=70mm and $\sigma_0 = 1.5 \times 10^8 Pa$. We here take the limit crack propagation velocity as $v = 0.4 C_R$=1106m/s. Then we can use Eq.(15) to conservatively evaluate the characteristic strain rate for the largest specimen with diameter 600 mm

$$\dot{\varepsilon}_{Ic} = \frac{\sigma_0 v(D)}{3GD(1 + D/D_0)^{1/2}} = 0.95 s^{-1}$$

In [18] for high strength concrete cylinders under the impact velocity of 7 m/s the real strain rates varied in the range of 0.014-0.111 s^{-1} that were well below the characteristic strain rate, therefore static size effect dominated the size effect of the high strength concrete cylinders, and the apparent strength decreased as the size of the specimen increased.

Obviously, static size effect also was a dominant factor in the tests in work [31].

Therefore, the proposed model interpreted the main features of the above mentioned tests, and explained the apparent controversy.

5. Concluding remarks

Rock-like materials have complex internal heterogeneous structure. The deformation and fracture of rocks also vary with time. Their temporal scales of changes are related to the internal structure and physical-mechanical properties of rocks. To understand the nature of dynamic size effect of strength of rocks it is necessary to consider the structural hierarchy of rocks and the temporal properties of deformation and fracture process of rocks. This paper establishes the relationship between strength, sample size and strain rate by adopting relaxation model of Maxwell type for rock. It has been shown that when the strain rate is well above certain characteristic strain rate the dynamic loading process takes predominant role due to the finiteness of crack propagation velocity. The larger the sample size is, the more time is needed for cracks to develop through the sample and the higher are the applied stresses before macrofracture. Factually the dynamic strength enhancement is caused by overloading induced by the delay of fracture due to the finiteness of the fracture propagation velocity. Because of the size effect of rock strength, the overloading will initiate the cracking at smaller scale levels of rock sample; hence the fragment size is smaller. Combining the size effect equations, the developed models succeeded in predicting the dynamic fragmentation size. As we showed the proposed fragmentation model applies with the model of Grady. The developed models also succeeded in predicting the characteristic transition strain rate and characteristic sample size. The mechanism underlying dynamic size effect on rock mass strength is examined, the main features and the apparent controversy in experimental data was explained, and the predominant parameters for static and dynamic size effect are clearly identified.

ACKNOWLEDGEMENT

The study was conducted with financial support of the National Natural Science Foundation of China (NSFC grants No. 51174012), the Project of Construction of Innovative Teams and Teacher Career Development for

Universities and Colleges Under Beijing Municipality(NoIDHT20130512), the “973” Key State Research Program (grant No. 010CB732003), Science Fund for Creative Research Groups of the National Natural Science Foundation of China（NSFC grant No. 51021001） We also thank Dr Q.M. Li from the University of Manchester for his valuable comments on this paper.

References

[1] Bazant ZP, Yu Q. Universal size effect law and effect of crack depth on quasi-brittle structure strength. J Eng Mech 2009; 135(2): 78-84.

[2] Weibull W. The phenomenon of rupture in solids. Proc., Royal Swedish Institute of Engineering Research (Ingenioersvetenskaps Akad. Handl.), 1939; 153:1-55

[3] Weibull W. A statistical theory of the strength of materials. Proc., Royal Swedish Academy of Engineering Science, 1939; 151:1-45.

[4] Weibull W. A statistical distribution function of wide applicability. J Appl Mech 1951; 18(3): 293-297.

[5] Bazant ZP. Size effect in blunt fracture: Concrete, rock, cracks. J Eng Mech 1984; 110 (4):518-535.

[6] Bazant ZP, Xi Y. Statistical size effect in quasi-brittle structure: II. Nonlocal theory. J Eng Mech 1991: 117(11): 2623-2640.

[7] Bazant ZP. Scaling of quasi-brittle fracture: asymptotic analysis. Int J Fract 1997; 83(1):19-40.

[8] Bazant ZP, and Novak D. Probabilistic nonlocal theory for quasibrittle fracture initiation and size effect. I: Theory. J Eng Mech 2000; 126(2): 166-174.

[9] Bazant ZP and Pang SD. Activation energy based on extreme value statistics and size effect in brittle and quasi-brittle fracture. J Mech Phys Solids 2007; 55(1): 91-134.

[10] Bazant ZP. Vorenchovsky M and Novak D. Asymptotic prediction of energetic-statistical size effect from deterministic finite-element solution. J Eng Mech 2007; 133(2):153-162.

[11] Bazant ZP, Kazemi MT. Determination of fracture energy, process zone length and brittleness number from size effect, with application to rock and concrete. Int J Fract 1990, 44(1): 111-131.

[12] Bazant ZP and Planas J. Fracture and size effect in concrete and other quasi-brittle materials, CRC Press, Roca Raton, Fla., Chap 12, 1998.

[13] Hu XZ, Duan K. Size effect and quasibrittle fracture: the role of FPZ. Int J Fract 2008; 154 (1-2): 3-14.

[14] Morel S. Size effect in quasibrittle fracture: derivation of the energetic size effect law from equivalent LEFM and asymptotic analysis. Int J Fract 2008; 154 (1-2): 15-26.

[15] Carpinteri A. Scaling law and renormalization group for strength and toughness of disordered materials. Int J Solids Struct 1994; 31: 291-302.

[16] Carpinteri A, Puzzi S. Self-somilarity in concrete fracture: size-scale effecte and transition between different collapse mechanisms. Int J Frac 2008; 154(1-2): 167-175.

[17] Carpinteri A, Pugno NM. Mechanics of hierarchical materials. Int J Fract 2008; 150 (1-2): 221-226.

[18] Krauthemerat T, Elfahala MM, Lim J et al. Size effect for high strength concrete cylinders subjected to axial impact. Int J Impact Eng 2003; 28(9):1001-1016.

[19] Elfahal MM, Krauthammer T. Dynamic size effect in normal-and high-strength concrete cylinders. ACI Mat J 2005, 102(2): 77-85.

[20] Elfahala MM, Krauthemerat T, Ohnob T et al. Size effect for normal strength concrete cylinders subjected to axial impact. Int Impact Eng 2005; 31(4): 461-481.

[21] Hong L, Li XB, Ma CD et al. Study on size effect of rock dynamic strength and strain rate sensitivity. Chinese J Rock Mech Eng 2008; 27(3): 526－533.

[22] Attewell PB. Dynamic fracturing of rocks, parts I, II, III, Colliery Engineering 1963; pp:203-10, 248-52, 289-94.

[23] Rinehart JS. Dynamic fracture strength of rock. Proceeding of 7th symp.on Rock Mech ALME, pp:205-208,1965.

[24] Kumar A. The effect of stress rate and temperature on the strength of basalt and granite. Geophysics 1968; 33(3): 501-510.

[25] Lindholm US, Yeakley LM and Nagy A. 1974. The dynamic strength and fracture properties of dresser basalt, Int J Rock Mech Mining Sci 1974; 11:181-191.

[26] Wang QZ, Zhang S and Xie HP. Rock Dynamic Fracture Toughness Tested with Holed-cracked Flattened Brazilian Discs diametrically impacted by SHPB and its size effect. Experimental Mechanics, 2010, 50:877-885.

[27] Gunsallus KL, Kulhawy FH. A comparative evaluation of rock strength measures. Int J Rock Mech Min Sci Geomech Abstr 1984, 21(5):233–248.

[28] Bhagat RB. Mode I fracture toughness of coal. Int J Min Eng 1985, 3:229–236.

[29] Whittaker BN, Singh RN, Sun G. Rock fracture mechanics: principles, design and applications. Elsevier, Amsterdam, 1992.

[30] Zhang ZX. An empirical relation between mode I fracture toughness and the tensile strength of rock. Int J Rock Mech Min Sci 2002, 39 :401–406

[31] Liang CY, Li X, Zhang H, Li SD, He JM, Ma CF. Research on size effect of uniaxial compression properties of granite under medium and low strain rates. Chinese J Rock Mech Eng 2013; 32(3): 528－536.

[32] Sherman SI, Seminsky KZ, Adamovich AN et al. Fault formation in lithosphere, zone of tension. Edited by Logachev N.A. Nauka, Novosibirsk, 1992.

[33] Radionov VN, Sizov IA, Tsvetkov VM. Fundamental of geo-mechanics. Nedra, Moscow, 1986.

[34] Landau LD, Lifshitz EM. Theory of elasticity. Pergamon, London, 1959.

[35] Fineberg J, Marder M. Instability in dynamic fracture. Phys Rep 1999; 313:101-108.

[36] Field JE, Walley SM, Proud WG et al. Review of experimental techniques for high rate deformation and shock studies. Int J Impact Eng 2004; 30(4): 725-75.

[37] Forrestal MJ, Wright TW, Chen W. The effect of radial inertia on brittle samples during the split Hopkinson pressure bar test. Int J Impact Eng 2007; 34(3): 405–11.

[38] Zhang M, Li QM, Huang FL et al. Inertia-induced radial confinement in an elastic tubular specimen subjected to axial strain acceleration, Int J Impact Eng 2010; 37(4): 459-464

[39] Li QM, Meng H. About the dynamic strength enhancement of concrete-like materials in a split Hopkinson pressure bar test. Int J Solids Struc 2003; 40(2):343-360.

[40] Li QM, Lu YB, Meng H. Further investigation on the dynamic compressive strength enhancement of concrete-like materials based on split Hopkinson pressure bar test, part II: numerical simulations. Int J Impact Eng 2009; 36(12): 1335-1345.

[41] Grady DE. Length scale and size distribution in dynamic fragmentation. Int J Fract 2010; 163: 85-99.

[42] Grady DE. Fragment size distribution from the dynamic fragmentation of brittle solids. Int J Impact Eng 2008; 35(12): 1557-1562.

[43] Achenbach JD. Wave propagation in elastic solids. North-Holland Publishing Company, Amsterdam, l973.